



**Wind Power Use Capacity in Rural Areas of Complex Topography via WRF Model: a Case Study in a Mountainous Region in Rio de Janeiro State, Brazil**  
Capacidade de Uso da Energia Eólica em Áreas Rurais de Topografia Complexa via Modelo WRF: um Caso de Estudo em uma Região Montanhosa do Estado do Rio de Janeiro, Brasil

Beatriz Rogers Paranhos<sup>1</sup>;  
Rafael Henrique Oliveira Rangel<sup>2</sup>; Reginaldo Ventura de Sá<sup>1</sup> & Marcio Cataldi<sup>1</sup>

<sup>1</sup>Universidade Federal Fluminense, Centro Tecnológico, Escola de Engenharia,  
Rua Passo da Pátria, 156 – Bloco D sala 133, 24210-240, Niterói, RJ, Brasil

<sup>2</sup>Universidade Federal do Rio de Janeiro, Instituto Alberto Luiz Coimbra de Pós-Graduação e Pesquisa de Engenharia,  
Laboratório de Métodos Computacionais em Engenharia (LAMCE),  
Av. Athos da Silveira Ramos, 149, Centro de Tecnologia, I-214, Cidade Universitária, 21941-909, Rio de Janeiro, RJ, Brasil  
Emails: beatrizparanhos@id.uff.br; rafael@lamma.ufrj.br; regis@lamma.ufrj.br; mcataldi@id.uff.br

Recebido em: 18/03/2019 Aprovado em: 16/05/2019

DOI: [http://dx.doi.org/10.11137/2019\\_3\\_52\\_63](http://dx.doi.org/10.11137/2019_3_52_63)

## Resumo

Estimulada por acordos ambientais globais, a busca por alternativas de geração de energia renovável vem aumentando em todo o mundo. Embora o Brasil tenha um grande território com diferentes recursos naturais, sua matriz energética é altamente dependente da fonte hidráulica. Este artigo avalia a capacidade de uso da energia eólica no topo de morros e montanhas, considerando o potencial eólico nesses locais e, assim, estimulando seu desenvolvimento no país. O modelo *Weather Research and Forecasting* (WRF) foi aplicado para identificar os recursos eólicos e definir os melhores locais para a instalação de aerogeradores na área da Cooperativa Agrícola de Vieira, localizada em Teresópolis, região montanhosa do estado do Rio de Janeiro, Brasil. Como pequenos aerogeradores operam próximos ao solo e, portanto, têm custos mais baixos do que os grandes, a produção estimada de eletricidade de um aerogerador nacional, de pequeno porte, foi comparada com o consumo real de uma lavoura de referência local. Apesar da fraca representação topográfica, os resultados mostram que a região possui recurso eólico suficiente para fornecer eletricidade aos agricultores ao longo do período estudado do ano, reduzindo seus custos de produção. Portanto, é possível melhorar o uso de energia eólica no Brasil em zonas montanhosas e, no processo, diversificar a matriz energética do país.

**Palavras-chave:** modelagem; regiões montanhosas; energia eólica

## Abstract

Encouraged by global environmental agreements, the search for renewable energy production alternatives has been increasing around the world. Although Brazil has a large territory with different natural resources, its energy matrix is highly dependent on the hydraulic source. This paper evaluates the wind power use capacity on the top of hills and mountains, considering the wind potential in these places and so stimulating its development in the country. The Weather Research and Forecasting (WRF) model was applied to identify the wind resource and to define the best sites to install aerogenerators in the area of the Agricultural Cooperative of Vieira, located in Teresópolis, a mountainous region in Rio de Janeiro state, Brazil. As small aerogenerators operate close to the ground, and so have lower costs than large ones, the estimated electricity production of a national aerogenerator was compared with the real consumption of a local reference tillage. Despite the poor topography representation, results show that the region has sufficient wind power to provide electricity to the agriculturists throughout the studied period of the year, reducing their production costs. Therefore, it is possible to improve Brazil's wind energy use in mountainous zones and in the process diversify the country's energy matrix.

**Keywords:** modeling; mountainous regions; wind energy

## 1 Introduction

The relevance of wind energy potential has increased in recent years in the global scenario due to its promising advantages. It is a renewable source, reduces the fossil fuel usage and reduces the greenhouse gases and other pollutants emission into the atmosphere. The wind, considered as a renewable source, is characterized by only low levels of indirect carbon emissions, being considered an interesting alternative for fossil fuels (Fang, 2014; Aso & Cheung, 2015). In Brazil, wind energy reached 7633 Mega Watts (MW) of installed capacity in 2015, resulting in a growth of 56.2% compared to 2014. Most investments were in the country's northeast coast, where the wind is frequent and reaches high velocities. Moreover, the South of Brazil is increasing its participation in the wind power generation, being the second biggest producer in the country. The Southeast has a little contribution to the sector, while the North and the Midwest still not generating electricity from wind power (EPE, 2016).

Despite Brazil's efforts to increase the use of wind energy in its large territory, its energy matrix is highly dependent on the hydraulic source. In 2015, it represented 64% of the total electricity generated, while wind energy represented 3.5% (EPE, 2016). The hydropower dependence reflects the great vulnerability in the Brazilian electricity sector. The bad management of water resources, of its usage's conflicts and of the dry periods can lead to water unavailability. In spite of being renewable, hydropower can cause significant impacts in its zone of influence, such as the alteration of the river's hydraulic characteristics and the interference in the aquatic and river-side environments. Besides that fact, in the Brazilian Northeast, the period of most intense winds are the dry months, so there is a complementation between periods of great wind power generation and great hydropower generation that can be largely explored (Dos Santos & Silva, 2013).

The airflow over hills increases speed at upstream and reaches its apex at the top (Stangroom, 2004). Therefore, the wind power in these regions has a promising potential for its energy use, but it is not commonly explored in Brazil. Considering

the country's extension, its wind potential and its expressive dependence on the hydraulic source, viability studies in mountainous regions for wind turbines implementation are relevant ways to develop this kind of activity in the country (Da Silva *et al.*, 2013; ABEEÓLICA, 2019).

The atmospheric modeling assists to determine the wind speed and direction in places where there are not any observed data to verify if these spots are able to produce wind energy. Furthermore, weather stations may possibly present some restraints, such as coarse resolution, data accuracy and also completeness and financial costs, as pointed by Al-Yahyai *et al.* (2010).

Modeling application examples are provided by Mattar & Borvarán (2016), who used the mesoscale atmospheric model Weather Research and Forecasting (WRF) to estimate the offshore wind potential in the central coast of Chile and concluded that wind power over the sea ranges between 745 and 1240 W m<sup>-2</sup>; Carvalho *et al.* (2012; 2014), who used WRF to simulate wind over Portugal, showing the impact of boundary layer parameterization and initial and boundary conditions choice in terms of wind energy production estimates; Giannaros *et al.* (2017) who also used WRF for simulating wind field over Greece for assessing wind resources and found a satisfactory model performance; and Lazić *et al.* (2014), who used the mesoscale model ETA with a new proposed MOS (Model Output Statistics) method to make wind forecast in Scandinavia and demonstrated its usefulness for wind energy applications.

Therefore, this paper aims to evaluate, via numerical modeling, the wind energy capacity in different altitudes, in the region near the Agricultural Cooperative of Vieira (CoopVieira), located in Teresópolis, Rio de Janeiro state, Brazil. There are family agriculture initiatives in this area, together with subsidized agriculture, which demands an expressive energy amount, mainly for irrigation services. Additionally, to value and stimulate the development of the wind energy industry in Brazil, the aerogenerator Verne 555, designed by the national company Enersud, was considered to estimate the electrical production over the area.

The use of sustainable technologies, such as wind energy applications in rural communities, reflects the possibility of reducing production costs related to energy consumption. The methodology developed in this study can also be used in other places in Brazil and the world that have these same complex topography and small-scale farming characteristics.

## 2 Material and Methods

### 2.1 Study Area Description

The city of Teresópolis has 770.601 km<sup>2</sup> and is in the Mountainous Region of Rio de Janeiro state, at an altitude of 871 m above sea level. The local climate is classified as tropical altitude and it is propitious for the agricultural production (IBGE, 2016). In fact, the city's farming contribution in the Gross Domestic Product (GDP) of the state in 2013 corresponded to 18% in this sector (IBGE, 2016). In the rural area of Teresópolis, the small landholdings managed by family agriculturists dominate.

The Agricultural Cooperative of Vieira (CoopVieira) is situated in Teresópolis between the km 33 and 45 of RJ-130 road. The Cooperative is com-

posed of forty-one familiar agriculturists and twelve non-agriculturists, totalizing fifty-three partners. The crop is predominantly of lettuce, chive, kale and watercress. The production is of industrial scale with a huge electricity consumption all over the year.

### 2.2 Aerogenerator Selection

To appraise and incite the development of the Brazilian wind turbine industry, as well as to provide an economically feasible solution, the aerogenerator Verne 555, designed by the national company Enersud, was selected for the study. It is Enersud's most powerful model with 6 kW of rated output power reached by 12.00 m.s<sup>-1</sup> of rated output speed. Verne 555's cut-in speed is equivalent to 2.20 m.s<sup>-1</sup>. It is constituted of a horizontal axis wind turbine in an upwind configuration (Enersud, 2016). To optimize the wind use capacity, the analyses were made considering the tallest tower fabricated by Enersud, measuring 18 m in height.

### 2.3 Model Application

The mesoscale model used is the Advanced Research Weather Research and Forecasting (WR-

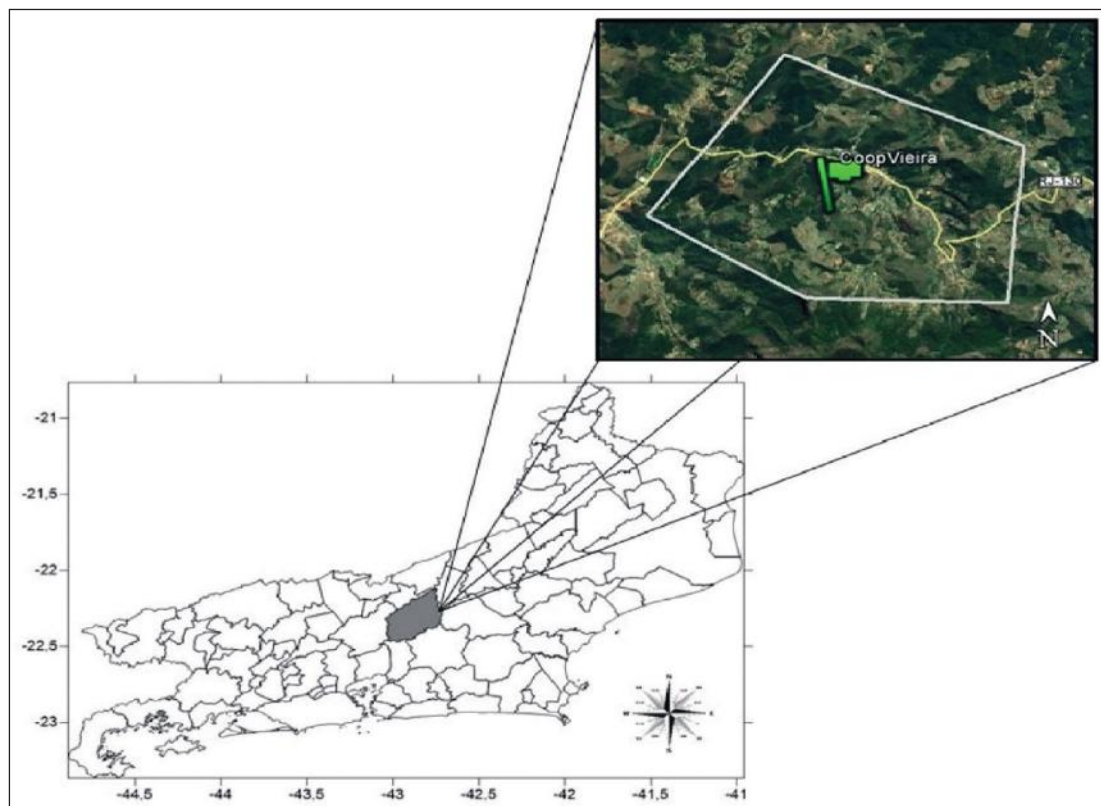


Figure 1 Study area: Rio de Janeiro state map and the Agricultural Cooperative of Vieira, in the city of Teresópolis.

F-ARW) modeling system version 3.6.1 (Skamarock *et al.*, 2008). The simulation was built with four grids using one-way nesting, centered between the closest weather station and the CoopVieira, in the  $-22.308372^\circ$  latitude and  $-42.698486^\circ$  longitude. Configured with Mercator map projection, the horizontal spatial resolutions adopted were of 27 km, 9 km, 3 km and 1 km (Figure 2). The study area consists of the last domain (d04). The dimensions of each of these domains were respectively 1620 x 1620 km<sup>2</sup>, 549 x 549 km<sup>2</sup>, 282 x 282 km<sup>2</sup> and 40 x 40 km<sup>2</sup>. Furthermore, the time step was set to 120 s and 47 vertical levels were used.

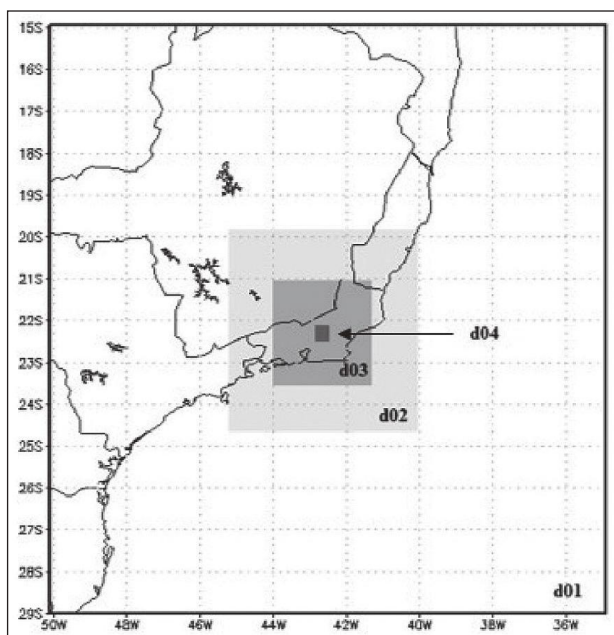


Figure 2 Nested grids with 27 km (d01), 9 km (d02), 3 km (d03) and 1 km (d04) of horizontal spatial resolution.

The initial and boundary conditions were obtained from the Global Forecast System (GFS) model 3-hour forecast files, for 48 hours forecast horizon, and a horizontal resolution of  $0.5^\circ$ . The topographic data collected from the United States Geological Survey (USGS) have been set to a resolution of 10 arcminutes for grid 1; 5 arcminutes for grid 2; 2 arcminutes for grid 3 and 30 arc seconds for grid 4. The parameterizations were chosen as suggested by Dragaud *et al.* (2018) and are summarized in Table 1.

In order to obtain a representative average result of the wind in the study area, this paper sought

Physic Process	Scheme	Reference
Microphysics	Goddard	Tao <i>et al.</i> , 1989
Longwave radiation	RRTM	Mlawer <i>et al.</i> , 1997
Shortwave radiation	Dudhia	Dudhia, 1989
Surface layer	MM5 Similarity	Paulson, 1970; Dyer & Hicks, 1970; Webb, 1970; Beljaars, 1994; Zhang & Anthes, 1982
Land surface	5-Layer Thermal Diffusion	Dudhia, 1996
PBL physics	MRF	Hong & Pan, 1996
Cumulus physics	Kain-Fritsch	Kain, 2004

Table 1 Parameterization schemes used in this study.

to work with weather systems that affect the airflow behavior in different modes, such as prefrontal, frontal, and low-pressure systems. Therefore, the simulations occurred in three distinct dates. On the first one, January 24<sup>th</sup> 2014, Rio de Janeiro state was in a prefrontal synoptic condition. On the second one, November 26<sup>th</sup> 2014, the state was in a low-pressure system and a frontal system passing through the ocean, approximately in São Paulo state's coast. Finally, the last date, December 22<sup>nd</sup> 2014, is characterized by presenting a cold front approaching Rio de Janeiro state and moving through it. The classification of the weather systems was made consulting satellite images and synoptic charts (INPE, 2016). In all cases, the simulations were configured to start at 0000 UTC and last 48 hours.

## 2.4 Wind Resource Determination

According to the model, in the d04 domain, the weather station's closest grid point is at 1408 m of altitude and the real weather station is, actually, at 1065 m. To this particular region, the WRF's topography had a poor reality representation in the highest resolution domain. Thus, there is a significant difference of 343 m between the real and the simulated position. Specifically, the WRF does not display that the weather station is effectively in a valley region (Figure 3). However, in the CoopVieira's area, WRF had a better topography representation.

An interesting place to install wind turbines in the CoopVieira is, as simulated by the model, at 1155 m of altitude but it is really at 1149 m of altitude, representing 6 m of difference.

The major problem involved with the poor topography representation consists of the unrealistic atmospheric process answers provided by the model. In other words, the wind variation is highly dependent on the topographic resolution used, mainly in mountainous regions (Stull, 1988; Bilal *et al.*, 2016). The WRF uses the USGS dataset, whose highest resolution option is equivalent to 30 arc seconds (about 1 km) (NCAR, 2016). The model was forced

to 5 arc seconds topographic resolution for grid 4, but it continued to show an erroneous topography lecture. In addition, the grid spatial resolution was changed to 10.8 km, 3.6 km, 1.2 km and 0.4 km, but the problem persisted.

The 30 arc seconds USGS's topography resolution may not be appropriate to a punctual definition of aerogenerators located in a mountainous region in Rio de Janeiro, as Teresópolis. Even so, it was feasible to estimate the average wind dynamic at altitude ranges of 100 m. Therefore, to the three simulated dates, the average wind speed vector and direction were calculated at 10 m height as well as

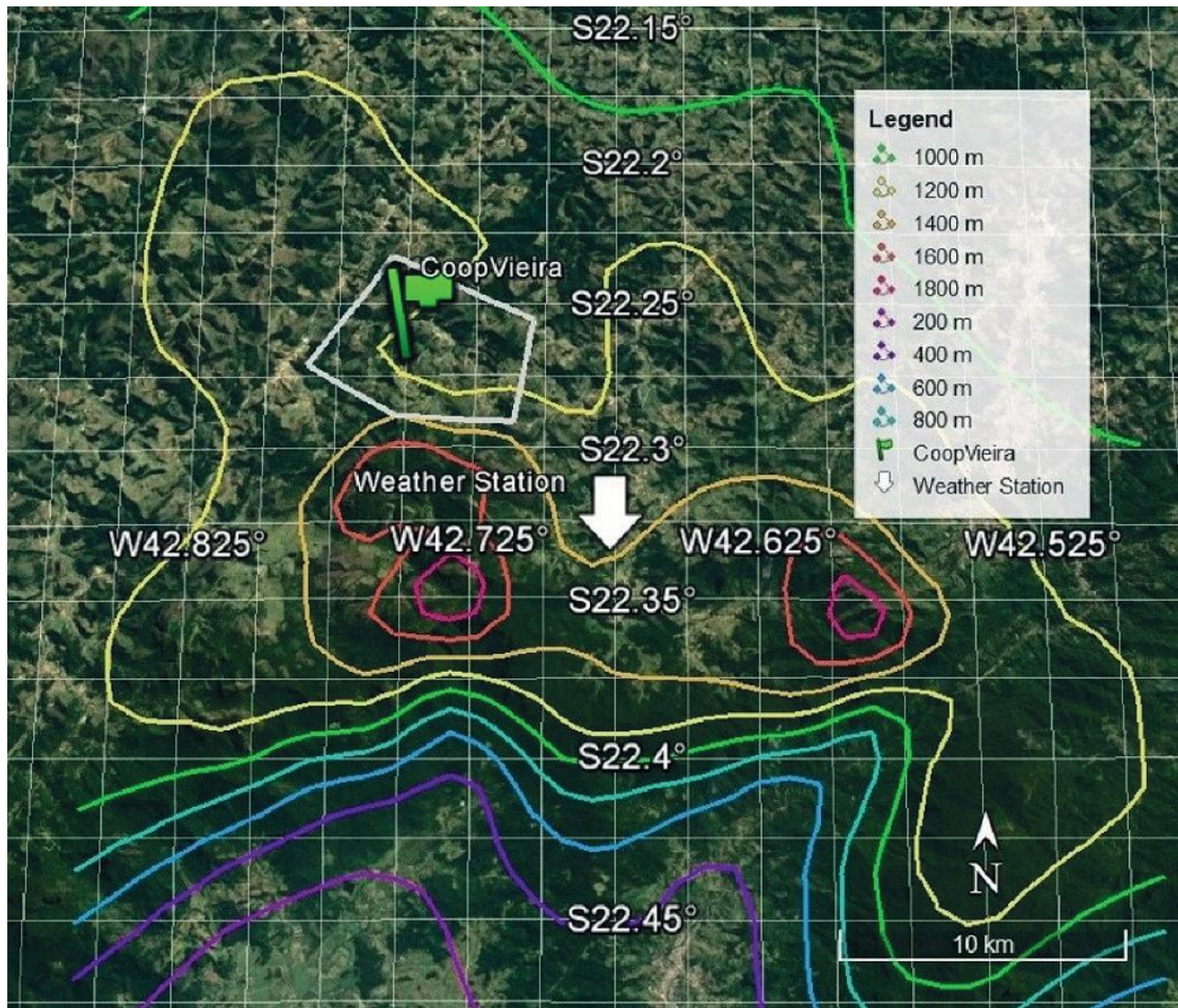


Figure 3 WRF contour plans superimposed on Google Earth satellite image.

the associated standard deviations. This procedure was executed considering the range of 1000 to 1100 m, 1100 to 1200 m, 1200 to 1300 m and 1300 to 1400 m.

The wind vertical profile for the three simulations and in each range was determined using the Law of the Wall, simplified solutions that calculate the wind speed in the turbulent sublayer (Cataldi, 2002). The Businger-Dyer relations (Businger *et al.*, 1971) for a neutral boundary layer (Stull, 1988) were applied due to the lack of turbulence parameters data near the surface (Equations (1) and (2)).

Considering that the three simulation dates are typical days of each month, the monthly average values of the friction velocity were obtained by equation (1). The Wind Atlas of the State of Rio de Janeiro (Amarante *et al.*, 2002) estimates the roughness length to be 1 m, as it is a rural zone in a mountainous terrain. The reference height was set to 10 m, the level where the model simulates the wind speed. Von Kármán constant is equal to approximately 0.4.

Equation (2) provides the wind speed data in function of the height  $u(z)$ . These data were calculated for the trimester of November, December and January and its average. These averages have enabled the provision of the wind vertical profile of the region. Similarly, it was used to discover the monthly standard deviations. This procedure enables the comparison between the average values summed and subtracted from one standard deviation (68.2% of a normal distribution), in order to define a normal operation range for a certain period and height of interest.

$$u_{\tau} = k\bar{u}_x(h_r)/\ln(h_r/z_0) \quad (1)$$

$$u(z) = u_{\tau}/k \ln(z/z_0) \quad (2)$$

## 2.5 Energetic Production

The probability density function  $f(u)$  of Weibull Distribution indicates the time fraction for which the wind has a certain velocity (equation (3)) (Mathew, 2006; Murthy & Rahi, 2016). The Wind Atlas of the State of Rio de Janeiro (Amarante *et al.*, 2002) provided the shape factor as being equal to 2. The scale factor  $c$  is represented by equation (4), which considers the *gamma* function  $\Gamma$  (Amarante *et al.*, 2002; Murthy & Rahi, 2016).

$$f(u) = k/c (u/c)^{k-1} \exp - (u/c)^k \quad (3)$$

$$c = \bar{u}/\Gamma(1 + 1/k) \quad (4)$$

The energetic production EP is estimated by the association of the aerogenerator power curve  $P(u)$ , in kW, with the probability density function (Equation (5)) (Mentis *et al.*, 2016). This study intended to find the monthly EP, so  $H$  corresponds to the number of hours in a month. The EP determination considered the normal wind speed distribution at 18 m height for each altitude range.

$$EP = H \int_{u_i}^{u_f} P(u)f(u)du \cong H \sum_{i=1}^N P(u_i)f(u_i)\Delta u_i \quad (5)$$

To evaluate the wind turbine performance considering the height and, consequently, the wind speed (Mathew, 2006), equation (6) defines the capacity factor CF of the Verne 555 (Mentis *et al.*, 2016; Watts *et al.*, 2016). This factor represents the ratio between the energy generated in local circumstances and the potential energy produced in a year by the machine rated power  $P_n$ . The annual energetic production AEP is considered using  $H$  as the number of hours in a year (equation (6)). For this purpose, the scale factor was calculated as an average wind velocity of the simulated studied period.

$$CF = AEP/8760 P_n \quad (6)$$

## 3 Results and Discussion

### 3.1 The Local Wind Dynamic

Visualization of the wind dynamic over the study area is relevant to comprehend how the air flows in this local situation. Figures 4, 5 and 6 show the wind behavior in the study area according to the model, despite the inadequate topography representation. They exhibit the contour plans and the streamlines at 10 m height in d04 at 1400 UTC for January 24<sup>th</sup> 2014, November 26<sup>th</sup> 2014 and December 22<sup>nd</sup> 2014, respectively. In the November simulation, wind has the highest velocities, mainly between -22.36 and -22.41 latitude and -42.85 and -42.55 longitude. This region is where WRF sees the steepest slopes. The other simulations present, with less impact, a similar behavior. Furthermore, in all

simulations, at downwind (South of the peaks), re-circulation zones and more turbulent wind patterns are observed, induced by the region's uneven topography. This type of analysis is important because it delimits, in function of the topographic distribution, the places with greater (upwind) and smaller (downwind) wind power generation potential in the area.

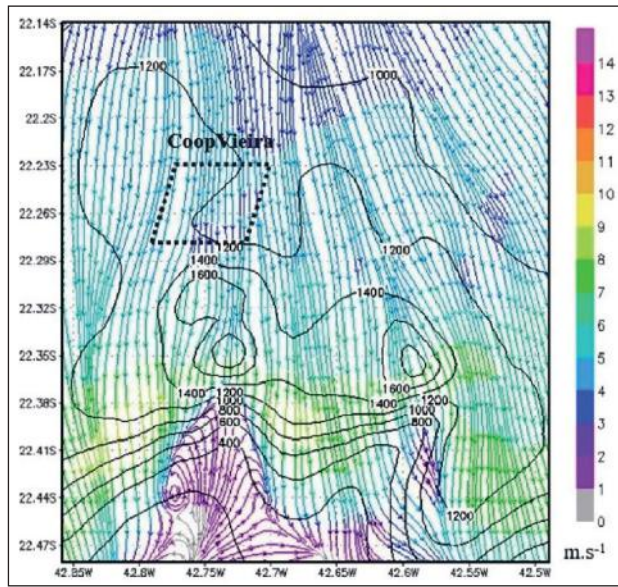


Figure 4 Wind behavior in the study area at 1400 UTC – 01/24/14.

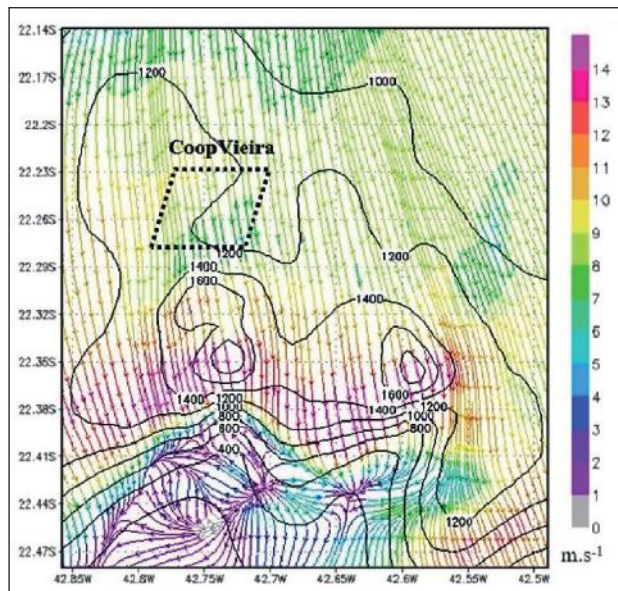


Figure 5 Wind behavior in the study area at 1400 UTC – 11/26/14.

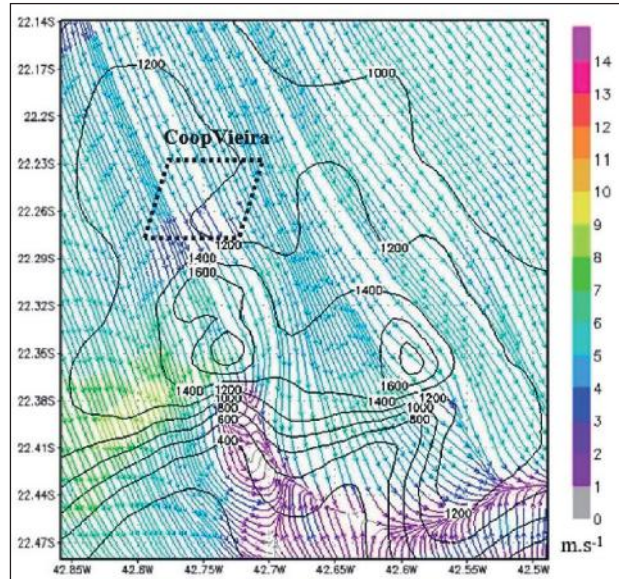


Figure 6 Wind behavior in the study area at 1400 UTC – 12/22/14.

### 3.2 Wind Speed and Direction Variability by Altitude Ranges

The mountains have an important role in air-flow behavior. Spots without obstacles have stronger wind velocities and fewer turbulence impacts (Stull, 1988). In mountainous regions, the higher hills are above the surface barriers. Figure 7 compares the monthly wind speed variability in the study area at 10 m height in different altitude ranges. Each column symbolizes the average wind velocity and the error bars are the respective standard deviations. For the three dates simulated, wind increases its average speed between 1000 and 1400 m. The average speeds in all situations are higher than the aerogenerator Verne 555's cut-in speed, showing the local wind resource capacity to generate energy during the analyzed period.

Figure 8 shows average wind speed at 10 m height measured by the closest weather station (-22.334839° latitude and -42.676932° longitude). In the same period of WRF simulation. The weather station is located at 1065 m height, represented in Figure 7 by the first class of altitude range (1000 – 1100 m). For the January 24<sup>th</sup> simulation, the difference between the average speeds of simulated and observed data in this range is about 1.02 m.s<sup>-1</sup>. For the November 26<sup>th</sup> simulation, this difference is about

2.11 m.s<sup>-1</sup>. Finally, for the December 22<sup>nd</sup> simulation, the difference is about 1.13 m.s<sup>-1</sup>. In all cases, WRF overestimates the values. This considerable difference between observed data and the model's results confirms the influence of topography representation in atmospheric modeling calculation.

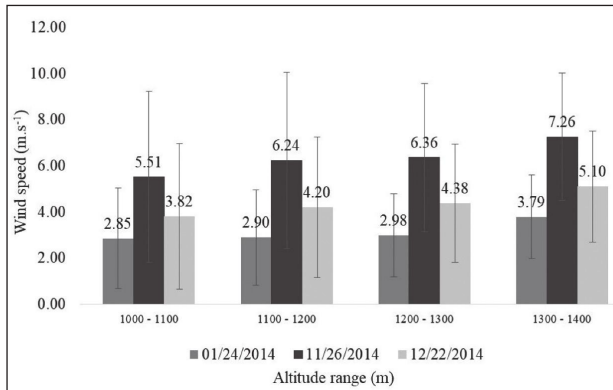


Figure 7 Wind speed at 10 m height per altitude range. For each range, the wind comparison between the January 24<sup>th</sup>, November 26<sup>th</sup> and December 22<sup>nd</sup> model simulations.

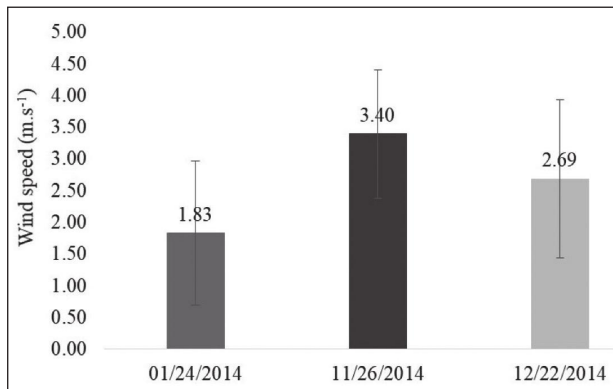


Figure 8 Average wind speed at 10 m height measured by the closest weather station in simulation dates.

Different airflow behaviors, in terms of average wind vertical profile for each altitude range studied, were found (Figure 9). The x-axis reproduces the average wind velocity and the y-axis symbolizes the height above the surface. From left to right, each line corresponds to a different altitude class: 1000 to 1100 m; 1100 to 1200 m; 1200 to 1300 m; 1300 to 1400 m. Thus, not only wind increases its intensity with the height above the ground, but also with altitude above sea level. Between 1300 to 1400 m, the wind has a significantly larger value, being more interesting for wind energy use in the area.

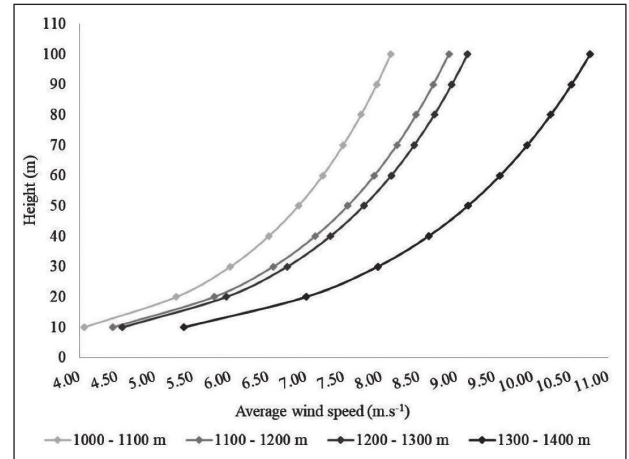


Figure 9 WRF's average wind vertical profile for different altitude ranges.

Wind direction is an important parameter to determine the wind turbine location on a wind farm. The machine's installation should be placed where there is a minimum number of obstacles in the prevailing wind direction (Stull, 1988). Table 2 shows the average and the standard deviation wind direction by altitude range and date simulated. In the study area, in all cases at 10 m height, the wind is predominantly from northwest, with variations between southwest and northeast. Table 3 represents the average and the standard deviation wind direction measured by the closest weather station, at 10 m height. January 24<sup>th</sup>-25<sup>th</sup> and December 22<sup>nd</sup>-23<sup>rd</sup> have average wind direction from northwest, similarly to WRF's results. However, in November 26<sup>th</sup>-27<sup>th</sup> wind is predominantly from north, differing from the model's simulation.

Wind Direction						
Altitude (m)	01/24/2014		11/26/2014		12/22/2014	
	Average (degrees)	σ (degrees)	average (degrees)	σ (degrees)	average (degrees)	σ (degrees)
1000 - 1100	147.25	96.99	111.56	57.42	132.40	72.60
1100 - 1200	132.82	83.38	109.51	50.92	126.05	60.35
1200 - 1300	135.32	69.69	112.11	32.63	128.72	52.47
1300 - 1400	127.29	63.43	108.63	14.66	128.23	54.42

Table 2 Wind direction by altitude range and simulated date.

Wind Direction					
01/24/2014		11/26/2014		12/22/2014	
average (degrees)	$\sigma$ (degrees)	average (degrees)	$\sigma$ (degrees)	average (degrees)	$\sigma$ (degrees)
143	115	90	52	143	99

Table 3 Wind direction measured by the closest weather station in simulation dates.

### 3.3 Wind Power Production

Estimating wind power production in a given place by a certain aerogenerator model provides an effective result of the local wind energy capacity use. Comparison with the agriculturists' energy consumption helps to evaluate the efficiency of a given wind power capacity to meet specific production needs. Therefore, Figure 10 displays the electricity furnished by Verne 555 at 18 m height in a normal range operation in the four studied altitude ranges. This energy production does not include the energetic system's loss.

The electricity production considering the average speed plus the standard deviation in the four altitude classes is capable of supplying the crop consumption. The analysis of the average speed for power generation indicates that it is partially capable to attend the agricultural demand in most cases: 1000 to 1100 m, 1100 to 1200 m and 1200 to 1300 m. In contrast, average speeds less standard deviations produce sufficient energy just in a short period at 1300 to 1400 m.

Results show that power increases with altitude, evidencing that between 1300 and 1400 m above sea level are the best sites to install wind turbines in the study area. At these altitudes, one wind turbine can provide energy, on average, for two properties like the analyzed one. In the best scenario, considering the average speeds plus the standard deviations, 7.32% of CoopVieira's forty-one agriculturists could be supplied by one single turbine with 6 kW of rated output power at 18 m above the surface. In other words, at least fourteen aerogenerators Verne 555 are required to compose a wind farm that completely serves the Cooperative. As each wind turbine Verne 555 costs around BRL 57,450.00, without the electrical equipment, the power inverter, installation ser-

vices, assembly and freight, the implementation price of this wind farm would be of BRL 804,300.00. Considering the average consumption of 505 kWh and that the tariff costs BRL 0.56649 per kWh, the fifty-three CoopVieira's partners can recover the initial investment in approximately four years and four months. Besides that, searching for a more complete sustainable cycle in agriculturists' production, the crop's practices optimization can also rise the local wind energy performance (De Guimarães *et al.*, 2017). Another possibility to improve the wind power use in the area would be the implementation of an aerogenerator that works in higher heights, where the wind tends to be more intense and, consequently, more kinetic energy could be converted in electricity.

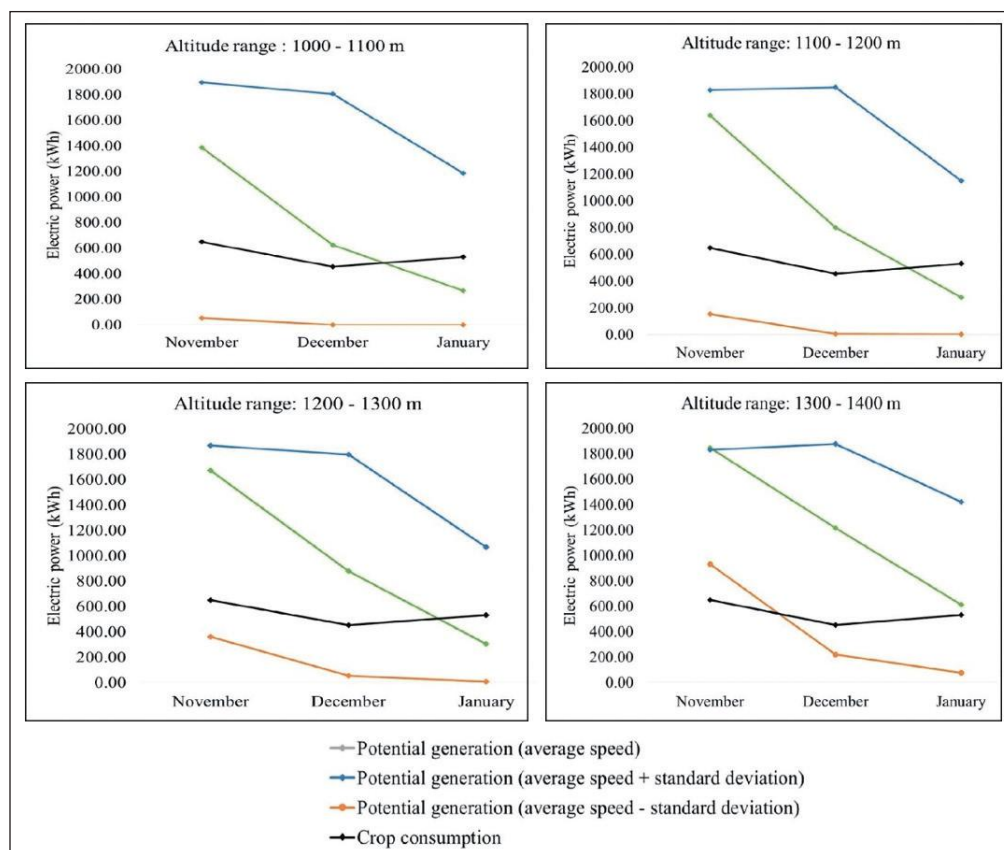
Regarding the Verne 555's capacity factor, Table 4 evidences its possible values in different altitudes for the average wind speed, the average wind speed plus the standard deviation and the average wind speed less the standard deviation. Once again, between 1300 and 1400 m, where the wind has the highest velocities, the capacity factor shows the best performance. Even between 1000 and 1100 m, where there is less wind power capacity, the capacity factor for the average wind velocity is expressive for a small wind turbine (Wiser *et al.*, 2012). In other words, Verne 555 represents an interesting machine in its category of small aerogenerators in the Brazilian market. However, it is still insufficient in terms of supply. Regardless of the quantity and the capacity of the wind turbines operating, the distributed generation is an interesting alternative to CoopVieira. The not consumed active power goes to the grid and can be transformed in power credits (kWh), representing reduction costs in the tillage productions (Brasil, 2012; Brasil 2015).

### 4 Conclusions

Results evidence that, between 1000 and 1400 m of altitude, the wind in the study area reaches enough speed to start and maintain wind power generation throughout the studied period. The altitude range from 1300 to 1400 m highlights the best sites for wind energy improvement. This finding allows the local agriculturists to have a second energy sour-

**Wind Power Use Capacity in Rural Areas of Complex Topography via  
WRF Model: a Case Study in a Mountainous Region in Rio de Janeiro State, Brazil**  
*Beatriz Rogers Paranhos; Rafael Henrique Oliveira Rangel; Reginaldo Ventura de Sá & Marcio Cataldi*

Figure 10 The electric power provided by Verne 555 at 18 m height and one of CoopVieira's tillage demand. The blue line represents the potential generation considering the average speed plus the standard deviation, the green line considers the average speed and the orange line the average speed subtracted by the standard deviation. In black, it is symbolized a CoopVieira's reference tillage with 1 ha area.



Capacity factor			
Altitude (m)	Average speed	Average speed + $\sigma$	Average speed - $\sigma$
1000 - 1100	0.17	0.42	0.00
1100 - 1200	0.21	0.43	0.00
1200 - 1300	0.22	0.42	0.02
1300 - 1400	0.30	0.43	0.08

Table 4 Capacity factor by altitude and wind speed configuration.

ce option, decreasing the dependence on energy provided by the distributor. Nevertheless, considering an aerogenerator like Verne 555, which has 18 m tower and 6 kW rated output power, working in the best wind scenario (not necessarily the real one) it would be necessary at least fourteen machines to totally supply the Cooperative's energetic demand.

The accurate selection of the best locations to install wind turbines by atmospheric modeling was unfeasible due to the low topography resolution in WRF and in GFS's initial and boundary conditions for wind power purposes. Teresópolis has a very irregular relief, with valleys and mountain peaks distributed in distances of less than 1 km, which would require a higher topography resolution than the one used in this study. This problem is relevant not only for wind project evaluations but also to extreme events forecasts, thus preventing disasters. In this context, to elaborate studies in regions with these characteristics, it is required to use WRF's newer versions and to employ a greater topographic resolution. The use of a subroutine to replace the current base topography in the model is also considered a solution, such as the Shuttle Radar Topography Mission (SRTM) application (Lupascu *et al.*, 2015). Besides that, to correctly run the model, it is necessary to apply a land use data file with compatible resolution.

The numerical simulation is a considerable resource for wind atlas elaboration in places with

precarious observed data stations, like Brazil, for example. However, to prepare this kind of research, as shown in this paper, it is necessary to use a very refined atmospheric modeling strategy, investigating not only the model's physics parameterizations but also the topography resolution. Without these methodological cares, a wind atlas may erroneously indicate areas with wind power potential use, especially in uneven topographies or very urbanized sites.

Given the region's lack of observed data and the poor topography representation in the WRF, this work served to have an order of magnitude of wind variation with altitude in the study area. It is possible to use wind energy in Brazilian mountainous regions when there are suitable support resources. This fact contributes to diversify the country's energetic matrix, using one of the most attractive renewable energy sources. Therefore, the investment in this technology expansion is totally worth, contributing to wind energy development in Brazil.

## 5 Acknowledgments

The authors would like to thank the Agricultural Cooperative of Vieira and the Enersud enterprise, fundamental actors for the development of this paper, as well as the financial help from the Conselho Nacional de Desenvolvimento Científico e Tecnológico (CNPq) - Projeto Universal No. 454397/2014-3 - MCTI/CNPQ 14/2014.

## 6 References

- ABEEÓLICA. 2019. Associação Brasileira de Energia Eólica. Available in: <[http://abeeolica.org.br/wp-content/uploads/2019/03/Infovento\\_PT.pdf](http://abeeolica.org.br/wp-content/uploads/2019/03/Infovento_PT.pdf)>. Accessed in: 13 mar. 2019.
- Al-Yahyai, S.; Charabi, Y. & Gastli, A. 2010. Review of the use of numerical weather prediction (NWP) models for wind energy assessment. *Renew and Sustainable Energy Reviews*, 14: 3192-3198.
- Amarante, O.A.C.; Silva, F.J.L. da & Rios Filho, L.G. 2002. *Atlas eólico do Estado do Rio de Janeiro*. Secretaria de Estado de Energia, da Indústria Naval e do Petróleo. Rio de Janeiro, Governo do Estado do Rio de Janeiro, 83p.
- Aso, R. & Cheung, W.M. 2015. Towards greener horizontal-axis wind turbines: analysis of carbon emissions, energy and costs at the early design stage. *Journal of Cleaner Production*, 87: 263-274.
- Beljaars, A.C.M. 1994. The parameterization of surface fluxes in large-scale models under free convection. *Quarterly Journal of the Royal Meteorological Society*, 121: 255-270.
- Bilal, M.; Birkelund, Y.; Homola, M. & Virk, M.S. 2016. Wind over complex terrain—Microscale modelling with two types of mesoscale winds at Nygårdsfjell. *Renewable Energy*, 99: 647-653.
- Brasil. Resolução Normativa ANEEL nº 482, de 17 de abril de 2012: Estabelece as condições gerais para o acesso de microgeração e minigeração distribuída aos sistemas de distribuição de energia elétrica, e dá outras providências. In: DIÁRIO OFICIAL DA REPÚBLICA FEDERATIVA DO BRASIL DE 19 DE ABRIL DE 2012. Brasília, 12p.
- Brasil. Resolução Normativa ANEEL nº 687, de 24 de novembro de 2015: Altera a Resolução Normativa nº 482, de 17 de abril de 2012, e os Módulos 1 e 3 dos Procedimentos de Distribuição – PRODIST. In: DIÁRIO OFICIAL DA REPÚBLICA FEDERATIVA DO BRASIL DE 2 DE DEZEMBRO DE 2015. Brasília, 25p.
- Businger, J.A.; Wyngaard, J.C.; Izumi, Y. & Bradley, E.F. 1971. Flux-profile relationships in the Atmospheric Surface Layer. *Journal of the Atmospheric Sciences*, 28: 181-189.
- Carvalho, D.; Rocha, A.; Gómez-Gesteira, M. & Santos, C. 2012. A sensitivity study of the WRF model in wind simulation for an area of high wind energy. *Environmental Modelling & Software*, 33: 23-34.
- Carvalho, D.; Rocha, A.; Gómez-Gesteira, M. & Santos, C. 2014. Offshore wind energy resource simulation forced by different reanalyses: comparison with observed data in the Iberian Peninsula. *Applied Energy*, 134: 57-64.
- Cataldi, M. 2002. *Simulação de Camadas Limites Estratificadas em Túnel de Vento*. Programa de Pós-graduação em Engenharia Mecânica, Instituto Alberto Luiz Coimbra de Pós-Graduação e Pesquisa de Engenharia, Universidade Federal do Rio de Janeiro, Master Dissertation, 102 p.
- Da Silva, N.F.; Rosa, L.P.; Freitas, M.A.V. & Pereira, M.G. 2013. Wind energy in Brazil: From the power sector's expansion crisis model to the favorable environment. *Renewable and Sustainable Energy Reviews*, 22: 686-697.
- De Guimarães, J.C.F.; Severo, E.A. & Vieira, P.S. 2017. Cleaner production, project management and Strategic Drivers: An empirical study. *Journal of Cleaner Production*, 141: 881-890.
- Dos Santos, A.T.S. & Silva, C.M.S. 2013. Seasonality, Interannual Variability, and Linear Tendency of Wind Speeds in the Northeast Brazil from 1986 to 2011. *The Scientific World Journal*, 2013: 1-10.
- Dragaud, I.C.D.V.; Silva, M.S.; Freitas Assad, L.P.; Cataldi, M.; Landau, L.; Elias, R.N. & Pimentel, L.C.G. 2018. The impact of SST on the wind and air temperature simulations: a case study for the coastal region of the Rio de Janeiro state. *Meteorology and Atmospheric Physics*, 121: 1-15.
- Dudhia, J. 1989. Numerical study of convection observed during the Winter Monsoon Experiment using a mesoscale two-dimensional model. *Journal of the Atmospheric Sciences*, 46: 3077-3107.
- Dudhia, J. 1996. A multi-layer soil temperature model for MM5. In: PREPRINTS, THE SIXTH PSU/NCAR MESOS-

**Wind Power Use Capacity in Rural Areas of Complex Topography via  
WRF Model: a Case Study in a Mountainous Region in Rio de Janeiro State, Brazil**  
*Beatriz Rogers Paranhos; Rafael Henrique Oliveira Rangel; Reginaldo Ventura de Sá & Marcio Cataldi*

- CALE MODEL USERS' WORKSHOP, 1996. Boulder, p. 22-24.
- Dyer, A.J. & Hicks, B.B. 1970. Flux-gradient relationships in the constant flux layer. *Quarterly Journal of the Royal Meteorological Society*, 96: 715-721.
- Enersud. 2016. Turbina Eólica Verne 555. Available in: <[http://enersud1.hospedagemdesites.ws/?page\\_id=147](http://enersud1.hospedagemdesites.ws/?page_id=147)>. Accessed in: 18 fev. 2016.
- EPE. 2016. Empresa de Pesquisa Energética. *Balanco Energético Nacional 2016 – Ano base 2015*. Rio de Janeiro. 62p.
- Fang, H.F. 2014. Wind energy potential assessment for the offshore areas of Taiwan west coast and Penghu Archipelago. *Renewable Energy*, 67: 237-241.
- Giannaros, T.M.; Melas, D. & Ziomas, I. 2017. Performance evaluation of the Weather Research and Forecasting (WRF) model for assessing wind resource in Greece. *Renewable Energy*, 102 (Part A): 190-198.
- Hong, S-Y. & Pan, H-L. 1996. Nonlocal boundary layer vertical diffusion in a medium-range forecast model. *Monthly Weather Review*, 24: 2322-2339.
- IBGE. 2016. Instituto Brasileiro de Geografia e Estatística. Available in: <<http://cod.ibge.gov.br/B6B>>. Accessed in: 11 fev. 2016.
- INPE. 2016. Instituto Nacional de Pesquisas Espaciais. Available in: <<https://www.cptec.inpe.br/>>. Accessed in: 7 jul. 2016.
- Kain, J.S. 2004. The Kain-Fritsch convective parameterization: An update. *Journal of Applied Meteorology*, 43: 170-181.
- Lazić, L.; Pejanović, G.; Živković, M. & Ilić, L. 2014. Improved wind forecasts for wind power generation using the Eta model and MOS (Model Output Statistics) method. *Energy*, 73: 567-574.
- Lupascu, A.; Iriza, A. & Dumitrache, R.C. 2015. Using a high resolution topographic data set and analysis of the impact on the forecast of meteorological parameters. *Romanian Reports in Physics*, 67(2): 653-664.
- Mathew, S. 2006. *Wind energy: fundamentals, resource analysis and economics*. Berlin, Springer, 246 p.
- Mattar, C. & Borvarán, D. 2016; Offshore wind power simulation by using WRF in the central coast of Chile. *Renewable Energy*, 94: 22-31.
- Mentis, D.; Syial, S.H.; Korkovelos, A. & Howells, M. 2016. A geospatial assessment of the techno-economic wind power potential in India using geographical restrictions. *Renewable Energy*, 97: 77-88.
- Mlawer, E.J.; Taubman, S.J.; Brown, P.D.; Iacono, M.J. & Clough, S.A. 1997. Radiative transfer for inhomogeneous atmospheres: RRTM, a validated correlated-k model for the longwave. *Journal of Geophysical Research*, 102: 16663-16682.
- Murthy, K.S.R. & Rahi, O.P. 2016. Preliminary assessment of wind power potential over the coastal region of Bheemunipatnam in northern Andhra Pradesh, India. *Renewable Energy*, 99: 1137-1145.
- NCAR. 2016. National Center for Atmospheric Research. Available in: <<http://www2.mmm.ucar.edu/wrf/users/>>. Accessed in: 12 jul. 2016.
- Paulson, C.A. 1970. The mathematical representation of wind speed and temperature profiles in the unstable atmospheric surface layer. *Journal of Applied Meteorology*, 9: 857-861.
- Skamarock, W.C.; Klemp, J.B.; Dudhia, J.; Gill, D.O.; Barker, D.M.; Duda, M.G.; Huang, X. & Powers, J.G. 2008. *A Description of the Advanced Research WRF version 3*. NCAR Technical Note, NCAR/TN-475+STR. National Center For Atmospheric Research. Boulder, 113p.
- Stangroom, P. 2004. *CFD modelling of wind flow over terrain*. Faculty of Engineering, Department of Civil Engineering, University of Nottingham, Ph.D. thesis, 298p.
- Stull, R.B. 1988. *An introduction to boundary layer meteorology*. Dordrecht, Kluwer Academic Publishers, 666p.
- Tao, W.; Simpson, J. & McCumber, M. 1989. An Ice-Water Saturation Adjustment. *Mon. Wea. Rev.*, 117: 231-235.
- Watts, D.; Oses, N.; Pérez, R. 2016. Assessment of wind energy potential in Chile: A project-based regional wind supply function approach. *Renewable Energy*, 96: 738-755.
- Webb, E.K. 1970. Profile relationships: The log-linear range, and extension to strong stability. *Quarterly Journal of the Royal Meteorological Society*, 96: 67-90.
- Wiser, R.; Lantz, E.; Bolinger, M. & Hand, M. 2012. Recent developments in the levelized cost of energy from U.S. wind power projects. Presentation February, 2012. 42p.
- Zhang, D.L. & Anthes, R.A. 1982. A high-resolution model of the planetary boundary layer— sensitivity tests and comparisons with SESAME-79 data. *Journal of Applied Meteorology*, 21: 1594-1609.